Temperature dependence of fast carbonyl backbone dynamics in chicken villin headpiece subdomain

Liliya Vugmeyster
Department of Chemistry and Environment and Natural Resources Institute, University of Alaska at Anchorage, 3211 Providence Drive, Anchorage, AK 99508, USA

Dmitry Ostrovsky
Department of Mathematical Sciences, University of Alaska at Anchorage, 3211 Providence Drive, Anchorage, AK 99508, USA

Abstract

Temperature-dependence of protein dynamics can provide information on details of the free energy landscape by probing the characteristics of the potential responsible for the fluctuations. We have investigated the temperature-dependence of picosecond to nanosecond backbone dynamics at carbonyl carbon sites in chicken villin headpiece subdomain protein using a combination of three NMR relaxation rates: $^{13}C'$ longitudinal rate, and two cross-correlated rates involving dipolar and chemical shift anisotropy (CSA) relaxation mechanisms, $13C'/^{13}C'-^{13}C^\alpha$ CSA/dipolar and $13C'/^{13}C'-^{15}N$ CSA/dipolar. Order parameters have been extracted using the Lipari-Szabo model-free approach assuming a separation of the time scales of internal and molecular motions in the 2–16°C temperature range. There is a gradual deviation from this assumption from lower to higher temperatures, such that above 16°C the separation of the time scales is inconsistent with the experimental data and, thus, the Lipari-Szabo formalism can not be applied. While there are variations among the residues, on the average the order parameters indicate a markedly steeper temperature dependence at backbone carbonyl carbons compared to that probed at amide nitrogens in an earlier study. This strongly advocates for probing sites other than amide nitrogen for accurate characterization of the potential and other thermodynamics characteristics of protein backbone.

Keywords

Protein dynamics; Temperature-dependence; Model-free; Chicken villin headpiece; NMR relaxation

Introduction

Temperature-dependence of protein dynamics can provide information on the details of the free energy landscape by probing the characteristics of the potential responsible for the fluctuations. (Cavanagh and Akke 2000; Wand 2001) This, in turn, provides means of determining various thermodynamics parameters such as configurational entropy and heat capacity, which play an important role in ligand-binding (Bracken et al. 1999), protein–

protein interactions, and protein stability(Jaenicke 2000; Schuler et al. 2002). NMR has an advantage of probing selective contributions from various parts of the protein depending on chosen isotopical labeling patterns and pulse sequences employed. Most of temperature-dependent NMR studies of backbone dynamics at picosecond-to-nanosecond time scale have been performed on amide nitrogens (Mandel et al. 1996; Yang et al. 1997; Seewald et al. 2000; Spyracopoulos et al. 2001; Vugmeyster et al. 2002; Idiyatullin et al. 2003; Massi and Palmer 2003; Krizova et al. 2004; Johnson et al. 2007).

NMR relaxation studies focused on amide nitrogen nuclei primarily probe fast picosecond motions of the N–H bond vector. However, they miss on other modes of motions of the peptide plane, particularly those that occur around an imaginary axis which is parallel to the N–H bond vector. (Wang et al. 2003b) Carbon nuclei at backbone carbonyl sites provide complimentary probes in this regard as they report on a different subset of motions, which is supported by studies on several proteins such as ubiquitin, ribonuclease binase, calmodulin, ribonuclease T1, and dematin headpiece C-terminal domain (Engelke and Ruterjans 1997; Pang et al. 2002; Wang et al. 2003b, 2005, 2006; Chang and Tjandra 2005; Vugmeyster et al. 2010) This implies a different local potential governing fast fluctuations of the N–H bond vectors versus the fluctuations of other atoms of peptide planes and reinforces the need for temperature-dependence studies at nuclei other than nitrogen in order to fully characterize the thermodynamic contribution of protein backbone to configurational entropy and heat capacity. The results of the study by Wang et al. (2003b) on ubiquitin and binase using $^{13}C'/^{13}C'-^{13}C^{\alpha}$ cross-correlated rate measurements indicated a remarkably strong temperature dependence of the carbonyl dynamics compared to dynamics at amide nitrogen sites. It is important to investigate whether these conclusions are applicable to other proteins and are supported by more refined methodologies.

To extract dynamical information from the NMR relaxation rates one needs a theoretical framework which relates the experimental rates to motional parameters. The most popular analysis of solution NMR relaxation studies is based on the model-free formalism of Lipari and Szabo and its extension by Clore et al. (Lipari and Szabo 1982; Clore et al. 1990) This treatment does not employ a specific model of motions and assumes an independence of internal fluctuations and overall tumbling of a molecule. This methodology has yielded many invaluable results and, importantly, has been applied to a large variety of proteins. As a result it allows for comparison among many different proteins and facilitates investigations of general principles governing backbone dynamics. The popularity of the approach is supported by its simplicity and the availability of standard pulse sequences for the measurements of laboratory frame relaxation rates at amide sites and computational tools for data analysis (Farrow et al. 1994; Orekhov et al. 1994; Mandel et al. 1995; Cole and Loria 2003). Limits of the validity of the model-free formalism, as well as alternative treatments and discussions have been recently presented (Vugmeyster et al. 2003; Frederick et al. 2008; Halle 2009; Meirovitch et al. 2009, 2010).

In this work we will investigate the temperature dependence of backbone dynamics at carbonyl sites in chicken villin headpiece subdomain(HP36). HP36 is a 36-amino acid helical thermostable protein that has been a subject of numerous experimental and theoretical studies due to its small size and fast folding rate (McKnight et al. 1996; Vugmeyster et al. 2002; Wang et al. 2003a; Brewer et al. 2005; Havlin and Tycko 2005; Kubelka et al. 2006; Tang et al. 2006; Wickstrom et al. 2006, 2007; Thurber and Tycko 2008; Vugmeyster and McKnight 2008; Vugmeyster et al. 2009; Xiao et al. 2009) Experimental temperature-dependence of the dynamics at amide nitrogen sites has been measured in an earlier study (Vugmeyster et al. 2002) and in the work by Massi and Palmer (2003) molecular dynamics simulations were used to obtain the temperature-dependent potential of mean force.

We will employ the experimental methodology similar to the one developed by Wang et al. (2006), which is based on the measurement of three relaxation rates: $^{13}C'$ longitudinal NMR relaxation rate R_1 and two cross-correlated rates involving dipolar and chemical shift anisotropy (CSA) relaxation mechanisms, $^{13}C'/^{13}C'-^{13}C^a$ CSA/dipolar and $^{13}C'/^{13}C'-^{15}N$ CSA/dipolar, denoted by $R_{C'/C'-C\alpha}$ and $R_{C'/C'-N}$, respectively. All three $^{13}C'$ relaxation rates are least sensitive to rotational fluctuations about an imaginary $C^\alpha-C^\alpha$ axis, a so-called crank-shaft motions(Bremi and Bruschweiler 1997), and most sensitive to rotational fluctuations about an imaginary axis parallel to the N–H bond direction, a so-called α-axis. This methodology is superior to the measurements based on the $R_{C'/C'-C\alpha}$ rates only, in particular because the order parameters extracted from this approach do not rely on the assumption of infinitely fast internal motions.

Our analysis will assume the separation of time scales of internal motions and overall tumbling and will demonstrate a remarkably stronger temperature-dependence of fast carbonyl dynamics compared to the one probed at the backbone nitrogen sites. We will also sho that our data provide an interesting example on the similarity of the time scales of the overall and internal motions for HP36 protein at temperature above ~16°C and, thus, illustrates the limit of the applicability of the Lipari-Szabo approach for the analysis of NMR relaxation rates.

Materials and methods

Sample preparation

$^{15}N/^{13}C$ labeled chicken villin headpiece subdomain sample was prepared according to the procedure described in Bi et al. (2006) The essence of the procedure consists of linking HP36 via a factor Xa cleavage sequence to the C-terminus of the N-terminal domain of the ribosomal protein L9. The following modifications were used: the protein was expressed in minimal media with 0.8 g/l ^{15}N NH$_4$Cl and 3 g/l ^{13}C-glucose. A G50 column (size 2 cm × 100 cm) with 20 mM Tris, 100 mM NaCl, 5 mM CaCl$_2$, and 0.01% azide buffer at pH 7.5 was used for a first purification step, followed by a cleavage by factor Xa. The cleavage was performed at room temperature with 8 units of factor Xa per mg of protein. The product was lyophilized and purified by Reverse-Phase HPLC. The identity and purity of the sample was confirmed by mass spectroscopy, N-terminal sequencing, ^{15}N NMR HSQC, and Reverse-Phase HPLC.

The protein was dissolved in 350 µl of 90% H$_2$O/10% D$_2$O to a concentration of 1.4 mM with 50 mM sodium acetate-D$_3$ buffer and the pH was adjusted to 5.4. A Shigemi tube made of susceptibility-matched glass was used.

NMR spectroscopy

As mentioned in the introduction, the strategy of Wang et al. (2006) used in our studies is based on the measurement of three relaxation rates: $^{13}C' R_1$, $R_{C'/C'-C\alpha}$ and $R_{C'/C'-N}$. All data were acquired on a 500 MHz Bruker NMR spectrometer equipped with triple resonance triple-gradient TXI probe. The measurement were taken at five temperatures, 2, 6, 12, 16, and 22°C with the temperature calibration performed using a deuterated methanol sample (Findeisen et al. 2007). For all three rates 512×40 complex points were acquired with the spectral width of 12 and 25 ppm in ^1H and ^{15}N dimensions, respectively. Recycle delay of 1.5 s was used. The data were processed by the NmrPipe/NmrDraw/NlinLS package (Delaglio et al. 1995). Each dimension was apodized by a 90° phase-shifted sine-bell window function and zero-filled once.

$^{13}C' R_1$ longitudinal relaxation rates were measured by a two-dimensional HN(CO) type pulse sequence(Kay et al. 1990) taking care to suppress cross-correlated mechanisms

involving N, H, and C^α nuclei with 180° pulses. Data with six relaxation delays between 0.01 and 1.4 s were recorded. The number of scans used was 24. The relaxation rates were obtained by fitting signal intensities to a mono-exponential decay. The uncertainties in rates were obtained by jack-knife simulations (Mosteller and Tukey 1977). $R_{C'/C'-C\alpha}$ and $R_{C'/C'-N}$ cross-correlated rates were measured using HN(CO) type pulse sequences described in Loth et al. (2005). The experiments are based on the principle of symmetrical reconversions (Pelupessy et al. 2003, 2007), which results in a more accurate measurements of cross-correlated relaxation rates than earlier techniques. Cross-correlation causes inter-conversions between two operators, in general denoted by P and Q. They are given by C'_y and $2C'_y C^\alpha_z$ operators for the $R_{C'/C'-C\alpha}$ experiment and C'_y and $2C'_y N_z$ operators for the $R_{C'/C'-N}$ experiment. Four measurements, denoted by I, II, III, and IV, are acquired in order to determine each cross-correlated rate. Experiment I measures the decay of P, IV the decay of Q, II the conversion $P \rightarrow Q$, and III the conversion $Q \rightarrow P$. The cross-correlated rate is extracted from the peak volumes of the four interleaved experiments as

$|R| = \frac{1}{T} \tanh^{-1} \sqrt{\frac{A_{II} A_{III}}{A_I A_{IV}}}$, where T is the relaxation delay time. The sign of the rate is determined by comparing the sign of intensities in the four experiments. The errors in the cross-correlated rates were estimated by assuming that errors in the intensity for each experiment are given by noise level in corresponding spectra. Data with the relaxation delay of 80 ms were acquired at all temperatures. An additional $R_{C'/C'-N}$ data set with the relaxation delay of 60 ms was collected for 22°C. 32 scans were used for experiments I and IV, and either 64 ($R_{C'/C'-C\alpha}$) or 128 ($R_{C'/C'-N}$) for experiments II and III.

The following residues had inherently lower intensities and, as a result, a reliable value for at least one of the cross-correlated rates could not be obtained at all temperatures: D44, D46, G52, M53, N60.

Determination of 13C′ order parameters

The experimental rates are fitted to corresponding spectral densities expressions to obtain effective $^{13}C'$ order parameters, local correlation times and directions of $^{13}C'$ CSA tensors. The expressions for the rates in terms of the spectral densities are given in references (Goldman 1984; Boyd et al. 1991; Brutscher et al. 1998; Fischer et al. 1998; Wang et al. 2006).

To parameterize the experimental rates we used the following model-free spectral density expression which assumes identical order parameters S^2 for all pairs of interactions a and b (Wang et al. 2006):

$$J^{ab} = \frac{2}{5} \left(\frac{S^2 \tau_c}{1 + (\omega \tau_c)^2} + \frac{(1 - S^2) \tau}{1 + (\omega \tau)^2} \right) P_2 \left(\cos \theta^{ab} \right). \qquad (1)$$

For auto-correlated terms $a = b$. P_2 is the second order Legendre polynomial and θ^{ab} is the angle between chosen components of the two interactions. $\tau = \frac{\tau_c \tau_e}{\tau_c + \tau_e}$, where τ^e reflects an average of local motions affecting a and b simultaneously. The interaction angles relevant to $R_{C'/C'-C\alpha}$ differ from angles relevant to the $R_{C'/C'-N}$ by the $C^\alpha - C' - N$ bond angle of 117°. Note that S^2 is related to the standard notation of the cross-correlated order parameter as $S^{ab} = S^2 P_2 (\cos \theta^{ab})$.

In addition to the relaxation rates, a list of isotropic $^{13}C'$ chemical shifts is required in order to estimate the components of carbonyl CSA tensor using the rules described in Loth et al. (Loth et al. 2005). It is also necessary to have the values of the overall tumbling time.

$^{13}C'$ assignments necessary for chemical shift estimates were previously obtained at 20°C (Vugmeyster and McKnight 2008). We have repeated the assignments at 8°C. The 8°C assignments were used for 2, 6, and 12°C temperatures, whereas the 20°C assignments were used for 16 and 22°C temperatures.

The values of S^2, τ_e, θ and h, the angle representing the orientation of σ_{11} axis (least shielded component) of $^{13}C'$ CSA tensor with respect to C'–C^α bond were obtained by a constrained (bounded) minimization of x^2 function in Matlab. Boundaries for the fitting parameters were as follows: $0 < S^2 < 1$, $\tau_c/1{,}000 < \tau_e < \tau_{e,max}$, $100° < \theta < 200°$. $\tau_{e,max}$, was selected as $\tau_c/2$ to obtain the main results of the paper, but varied for checks and validations. The standard Matlab routine for bounded minimization *fminbnd* only allows for a one-dimensional minimization (Brent 1973; Forsythe et al. 1976). For several dimensions the specific order of minimizations has to be chosen. We have used the following sequence: $\min_{\tau_e} \min_{S}{}^2 \min_\theta x^2 (\tau_e, S^2, \theta)$. In practice, the specific order did not matter. Several other orderings led to results coinciding with the initial one within the accuracy of the algorithm. For practical purposes, actual minimization was done over $\ln(\tau_e)$. The possibility of another minimum of x^2 was ruled out by inspection of $x^2(\tau_e)$ with fixed values of τ_e while minimizing with respect to S^2 and θ. This choice was made based on the observation of Wang et al. (2006) that when there are two minima their positions vary substantially in τ_e values. A second minimum in $x^2(\tau_e)$ was not observed for any residue.

The validity of the fitting procedure was confirmed by constructing synthetic data sets of rates from a range of S^2, τ_e, and τ_c values using the spectral density of the form specified by Eq. 1 and confirming that the algorithm returns the original values of these parameters. The parameters were taken as $S^2 = 0.95, 0.9, 0.8, 0.7$; $\tau_e = \tau_c/2, \tau_c/3, \tau_c/5, \tau_c/10, \tau_c/50$ for τ_c of either 3 or 5 ns; $C_{iso} = 175$ ppm and $\theta = 155°$. "Experimental errors" were specified as 3, 5, and 7% of the average values to the synthetic R_1, $R_{C'/C'-C\alpha}$ and $R_{C'/C'-N}$, respectively; these percentages are close to the average of actual experimental errors. x^2 minimization led to the exact reproduction of initial S^2 values with simulated errors in 0.03–0.05 range.

The following residues had to be excluded due to large x^2 values: K65 at 2°C, F47 and V50 at 6°C, and A59, K73 at 16°C. In addition, residues with data available for less than three temperature points were excluded from the analysis of the temperature dependence. A total of 26 residues were used in the analysis.

Results and discussion

Temperature dependence of carbonyl order parameters is much stronger compared to its backbone nitrogen counterpart.

Generalized order parameters at amide nitrogen sites have been previously obtained in the range of temperatures between 2 and 32°C for HP36 (Vugmeyster et al. 2002), at which the protein is at least 99% folded (McKnight et al. 1996). HP36 has been previously shown to tumble isotropically and the molecular tumbling times were determined on a ^{15}N labeled sample. The latter were shown to be consistent with the Stokes-Einstein relationship if 1.5 layers of hydration is included. Thus, we can use this approach to adjust the molecular tumbling times for the $^{13}C/^{15}N$ sample, which yields the values of 4.97, 4.36, 3.64, 3.11, and 2.65 ns for 2, 6, 12, 16, and 22°C, respectively.

Our initial goal was to investigate backbone carbonyl dynamics over the whole 2–32°C range, however, due to the small tumbling times the values of the smallest relaxation rate, $R_{C'/C'-N}$, could not be measured reliably above about 22°C. In addition, as will be shown and discussed in detail in the next section, the separation of time scales of the overall and internal motions, and, thus, the validity of the Lipari-Szabo approach could not be assumed for the data at 22°C. We have therefore obtained the order parameters at four temperatures, 2, 6, 12, and 16°C.

As elaborated in Materials and Methods Section, the values of effective order parameters S^2 at carbonyl sites, as well as internal correlation times τ_e and the angles θ representing the orientation of σ_{11} axis (least shielded component) of $^{13}C'$ CSA tensor with respect to C' $-C^\alpha$ bond vector are obtained by fitting three experimental relaxation rates to the spectral density of the form of Eq. 1, according to the approach developed by Zuiderweg and coworkers (Wang et al. 2006). The amplitude of local fluctuations for all interactions contributing to the three experimental rates at each site is assumed to be the same, and is thus reflected in a single effective value of the $^{13}C'$ order parameter. The fits were constrained by $\tau_e < \tau_c = 2$ under the assumption of the separation of the time scale of the molecular and internal motions. This constraint is somewhat arbitrary and its significance will be discussed in the following section.

The values of effective order parameters obtained from the experimental rates are shown in Fig. 1 for 2, 6, 12, and 16°C. A much stronger temperature dependence is observed compared to the amide nitrogen data. The average difference in carbonyl order parameters between 2 and 16°C is 0.18 ± 0.05, while it is 0.029 ± 0.015 for the nitrogen order parameters in the same temperature range.

To quantify the temperature dependence of order parameters we look at the slopes of plots of 1-S versus T. The meaning of the slope is easiest to see if we consider motions which are restricted to small excursions within an axially symmetric parabolic potential. In this case (Mandel et al. 1996), $\frac{d(1-S)}{dT} = \frac{3}{2}\frac{d<\alpha^2>}{dT}$, where α is the fluctuating angle. For other types of potentials the slopes 1 - S versus T provide a measure of temperature dependence in a selected temperature interval. The results are presented in Fig. 2 and Table 1. The resulting weighted average value is $4.9 \times 10^{-3} \pm 2 \times 10^{-4}$ 1/K, which is over 2.5 times larger than the value obtained from the backbone nitrogen data, $1.81 \times 10^{-3} \pm 6 \times 10^{-5}$ 1/K. Note that there are substantial variations among the residues (see SI5 for 1 - S versus T plots for all amino acids) and for six residues, F51, A59, L63, K65, N68, and L75 the temperature-dependence is not discernible within the error limits. The quality of the data is not sufficient to judge whether this is due to actual physical differences or insufficient precision.

Our results support the conclusion reached by Zuiderweg and coworkers (Wang et al. 2003b) regarding the temperature-dependence of carbonyl backbone motions in ubiquitin and binase on the basis of $R_{C'/C'-C\alpha}$ rates measurements. A substantially larger temperature dependence of backbone carbonyl order parameters indicates the necessity of probing multiple nuclei of the peptide plane in order to calculate the potential and other thermodynamic characteristics of protein backbone.

The deviation from the decoupling approximation gradually increases and the assumption of time scale separation is not valid for the rates above ~16°C.

The commonly used Lipari-Szabo model (1982) for the analysis of relaxation data in macromolecules and its extension by Clore and coworkers (1990) represent a macroscopic phenomenological approach in which the correlation function describing NMR relaxation is

parameterized by model-independent parameters, such as order parameters describing the amplitudes of motions and correlation times describing the time scales of motions. This approach uses a well-known decoupling approximation in which molecular and internal motions give independent contributions into the correlation function. The decoupling assumption is likely to break down when the ratio of correlation times for internal and overall motions, τ_e/τ_c; is not considerably smaller than 1. Several approaches have been developed that take into account correlations between the overall and internal motions (Meirovitch et al. 2009) and it has been shown that the Lipari-Szabo approach overestimates the values of the order parameters. This result has been obtained in a microscopic Slowly Relaxing Local Structure model by Tugarinov and coworkers (2001), as well as in a macroscopic phenomenological description by Vugmeyster et al. (2003) The latter approach estimates the upper limit of the correction to the order parameters is given by the factor of $\tau_c/(\tau_c - \tau_e)$; note, that this approach still requires a separation of the time scales of the overall and internal motions.

Correlation times at backbone nitrogen sites are usually short, as a result in order to see the deviations from the Lipari-Szabo assumption a sophisticated analysis of the data would be necessary. In contrast, as have been seen in a number of works, internal correlation times at backbone carbonyl sites tend to be much longer, on the order of 500–1,000 ps or larger, and thus the deviations for the decoupling assumption should be more significant. If the size of the protein under consideration is about 5 kDa, the separation of the time scales of the molecular and internal motions can approach the limit at which the model-free approach is not valid.

The small size of HP36 with the correlation time for overall tumbling of about 2.7 ns at 22°C makes it a good candidate for a direct observation of the limit of applicability of the decoupling approximation. As we will show below, the separation of the time scales is no longer valid for carbonyl motions at temperatures above 16°C.

The most straightforward assessment of the separation of the time scales would be based on reliable values of τ_e. Yet for the majority of the residues the fit of the relaxation rates to the spectral densities of Eq. 1 have not yielded reliable τ_e values, as indicated by very large uncertainties and the values falling on the upper boundary given by $\tau_c/2$. For lower temperatures this is likely due to the fact that for most residues the values of the order parameters are close to unity, and thus the fits to Eq. 1 are not sensitive to the values of τ_e. For higher temperatures, this is due to the fact that the fits can not fix the value of τ_e for a large ratio of τ_e/τ_c. To analyze this issue in detail we have generated a synthetic data set for the τ_c value of 3.65 ns, corresponding to the tumbling time of HP36 at 12°C, S^2 values in the range of 0.6–0.9, and with τ_e varied from 0.1 to 0.5 multiples of τ_c. The synthetic data were then re-fitted to Eq. 1. The results indicate that no reliable values can be expected for τ_e values when the ratio τ_e/τ_c reaches a certain threshold: $\tau_e/\tau_c<0.3$ for $S^2 = 0.6$, $\tau_e/\tau_c < 0.2$ for $S^2 = 0.8$, and $\tau_e/\tau_c < 0.1$ for $S^2 = 0.9$. However, the values of the order parameters can be determined with a reasonable accuracy even for large τ_e/τ_c ratios. The analysis, presented in detail in Supporting Information SI1, suggests that for the majority of residues at temperatures above 6°C the values of τ_e are larger than $0.2\tau_c$.

We think that the fact that the time scale of carbonyl motions is so much longer than that of N–H vectors for the whole temperature range points to the conclusion that the motions of the N–H bond vectors are dominated by fast proton fluctuations, either inside or outside the peptide plane, in which the rest of the nuclei of the peptide plane are not involved. In contrast, the motions of the carbonyl carbons contributing to the relaxation rates are likely to coincide with the motion of the peptide plane as a whole.

We have done the following check to further assess the stability of the fitted order parameters and the validity of the assumption of the separation of the time scales: we looked at the changes in S^2 values when the upper boundary constraining the allowable values of τ_e was varied from $\tau_c/3$ to $\tau_c/2$, as well as at the changes in corresponding χ^2 values. There is a trend from the lower to upper temperatures to make S^2 values more and more sensitive to the chosen τ_e upper boundary (first row of Table 2). Though χ^2 values are acceptable for all temperatures for $\tau_e < \tau_c/2$ boundary (second row of Table 2), they rise more sharply for higher temperatures when the boundary is lowered (third row of Table 2). This suggests that τ_e is approaching $\tau_c/2$ and the decoupling approximation becomes questionable. This trend also implies that the temperature dependence of τ_e is much less than that of τ_c. At 22°C the molecular tumbling time is 2.7 ns and the τ_c/τ_c ratio must be large enough to render the correlation function sensitive to the details of molecular motion and, thus, the Lipari-Szabo approach can no longer be applied.

We note that the values of θ are robust to variations in τ_e boundary. Fitted values of θ (SI3) do not differ across 2–16°C temperature range within the experimental errors, as expected for the folded state. Also the changes in the values of the order parameters are negligible if the angles θ are fixed as the average values reported in Table SI3. This is in part due to the fact that the rates R_1 do not depend on θ and, being the rates with the smallest experimental errors, they impose the most stringent constraints on the values of S^2 and τ_e.

One could argue that there are a number of assumptions inherent in Eq. 1, the most prominent being the assumption of the same order parameters for all interactions contributing to the carbonyl relaxation rates, which, in turn, implies isotropic local motions. Due to the fact that this approach has worked relatively well for several other proteins (Wang et al. 2006; Vugmeyster et al. 2010) at room temperature with similar amplitudes of fast motions to the ones seen for HP36 at 16°C, it is unlikely that the assumption plays an important role in the temperature-dependent trend that we observe.

Importantly, the correction to the decoupling approximation, discussed above, would make the temperature dependence of the carbonyl order parameters in the 2–16°C temperature range even larger, as the values of the order parameters are expected to be overestimated by a larger extent at higher temperatures. Even though we can not calculate these corrections quantitatively due to large uncertainties in the values of τ_e, the corrections would increase the values of the slopes of $1 - S$ versus T slopes, thus strengthening the main conclusion regarding the temperature dependence of the carbonyl dynamics.

One of the alternative approaches to the analysis of the experimental rates would be not to constraint the fits to Eq. 1 by the condition $\tau_e < \tau_c/2$: This would allow for a wider range of possibilities for both the order parameters and internal correlation times. Figure 3 displays a representative plot showing a range of allowable values of the order parameters and internal correlation times without any constraint on τ_e. We observe that for large values of τ_e there is a range of values of the order parameters and correlation times that fit the experimental data, which is consistent with a general behavior of the Lipari-Szabo type spectral densities. While this approach may yield statistically better fits, the meaning of the fitted parameters will not be the same as in the conventional model-free approach and its interpretation will require a consideration of a coupling between the internal and the overall motions. We, therefore, decided to constraint our analysis with the assumption of the separation of the time scales for the overall and molecular motions.

Conclusion

We have looked at the temperature dependence of the order parameters of fast motions at carbonyl carbon backbone sites in HP36 protein and compared it to an earlier study of amide nitrogen order parameters. The order parameters were obtained in 2–16°C temperature range using the model-free spectral density and assuming (a) that the amplitudes of local fluctuations for all interactions contributing to the three experimental rates are the same and (b) the separation of the time scales of molecular and internal motions, reflected in imposing the constraint on the fitting procedure as $\tau_e < s\tau_c/2$

While there are variations among the residues, on the average the carbonyl sites show a markedly steeper temperature dependence. The values of slopes in $1 - S$ versus T plots are on the average ~2.5 larger compared to the values obtained for the nitrogen sites. The results emphasize the need to probe nuclei other than nitrogen for accurate determination of the protein backbone potential and thermodynamic characteristics.

The small size of HP36 protein coupled to relatively long and weakly temperature-dependent values of internal correlation times led to an observation of the limit of the applicability of the decoupling approximation in the Lipari-Szabo model-free approach. As the temperature is raised and the molecular tumbling time decreases, the analysis of the data indicates a gradual deviation from the decoupling approximation. Above ~16°C the separation of time scales can no longer be assumed, at which point the model-free formalism can not be applied. While the importance of the separation of the time scales for the Lipari-Szabo approach has been discussed in a number of works, to our knowledge this work is the first to present the experimental evidence that the separation can fail for fast motions of the backbone.

Supplementary Material

Refer to Web version on PubMed Central for supplementary material.

Acknowledgments

References

Bi Y, Tang YF, Raleigh DP, Cho JH. Efficient high level expression of peptides and proteins as fusion proteins with the N-terminal domain of L9: application to the villin headpiece helical subdomain. Protein Expr Purif. 2006; 47:234–240. [PubMed: 16325421]

Boyd J, Hommel U, Krishnan VV. Influence of cross-correlation between dipolar and chemical-shift anisotropy relaxation mechanisms upon the transverse relaxation rates of N-15 in macromolecules. Chem Phys Lett. 1991; 187:317–324.

Bracken C, Carr PA, Cavanagh J, Palmer AG. Temperature dependence of intramolecular dynamics of the basic leucine zipper of GCN4: implications for the entropy of association with DNA. J Mol Biol. 1999; 285:2133–2146. [PubMed: 9925790]

Bremi T, Bruschweiler R. Locally anisotropic internal polypeptide backbone dynamics by NMR relaxation. J Am Chem Soc. 1997; 119:6672–6673.

Brent, RP. Algorithms for minimization without derivatives. Prentice Hall; Englewood Cliffs: 1973.

Brewer SH, Vu DM, Tang YF, Li Y, Franzen S, Raleigh DP, Dyer RB. Effect of modulating unfolded state structure on the folding kinetics of the villin headpiece subdomain. Proc Natl Acad Sci USA. 2005; 102:16662–16667. [PubMed: 16269546]

Brutscher B, Skrynnikov NR, Bremi T, Bruschweiler R, Ernst RR. Quantitative investigation of dipole-CSA cross-correlated relaxation by ZQ/DQ spectroscopy. J Magn Reson. 1998; 130:346–351. [PubMed: 9500898]

Cavanagh J, Akke M. May the driving force be with you—whatever it is. Nat Structr Biol. 2000; 7:11–13.

Chang SL, Tjandra N. Temperature dependence of protein backbone motion from carbonyl C-13 and amide N-15 NMR relaxation. J Magn Reson. 2005; 174:43–53. [PubMed: 15809171]

Clore GM, Szabo A, Bax A, Kay LE, Driscoll PC, Gronenborn AM. Deviations from the simple 2-parameter model-free approach to the interpretation of N-15 nuclear magnetic-relaxation of proteins. J Am Chem Soc. 1990; 112:4989–4991.

Cole R, Loria JP. FAST-Modelfree: a program for rapid automated analysis of solution NMR spin-relaxation data. J Biom NMR. 2003; 26:203–213.

Delaglio F, Grzesiek S, Vuister GW, Zhu G, Pfeifer J, Bax A. NMRPipe: a multidimensional spectral processing system based on UNIX pipes. J Biom NMR. 1995; 6:277–293.

Engelke J, Ruterjans H. Backbone dynamics of proteins derived from carbonyl carbon relaxation times at 500, 600 and 800 MHz: application to ribonuclease T1. J Biom NMR. 1997; 9:63–78.

Farrow NA, Muhandiram R, Singer AU, Pascal SM, Kay CM, Gish G, Shoelson SE, Pawson T, Forman-Kay JD, Kay LE. Backbone dynamics of a free and phosphopeptide-complexed Src homology 2 domain studied by 15N NMR relaxation. Biochemistry. 1994; 33:5984–6003. [PubMed: 7514039]

Findeisen M, Brand T, Berger S. A H-1-NMR thermometer suitable for cryoprobes. Magn Reson Chem. 2007; 45:175–178. [PubMed: 17154329]

Fischer MWF, Majumdar A, Zuiderweg ERP. Protein NMR relaxation: theory, applications and outlook. Prog Nucl Magn Reson Spectrosc. 1998; 33:207–272.

Forsythe, GE.; Malcolm, MA.; Moler, CB. Computer methods for mathematical computations. Prentice Hall; Englewood Cliffs: 1976.

Frederick KK, Sharp KA, Warischalk N, Wand AJ. Re-evaluation of the model-free analysis of fast internal motion in proteins using NMR relaxation. J Phys Chem B. 2008; 112:12095–12103. [PubMed: 18759409]

Goldman M. Interference effects in the relaxation of a pair of unlike spin-1/2 nuclei. J Magn Reson. 1984; 60:437–452.

Halle B. The physical basis of model-free analysis of NMR relaxation data from proteins and complex fluids. J Chem Phys. 2009; 131

Havlin RH, Tycko R. Probing site-specific conformational distributions in protein folding with solid-state NMR. Proc Natl Acad Sci USA. 2005; 102:3284–3289. [PubMed: 15718283]

Idiyatullin D, Nesmelova I, Daragan VA, Mayo KH. Heat capacities and a snapshot of the energy landscape in protein GB1 from the pre-denaturation temperature dependence of backbone NH nanosecond fluctuations. J Mol Biol. 2003; 325:149–162. [PubMed: 12473458]

Jaenicke R. Do ultrastable proteins from hyperthermophiles have high or low conformational rigidity? Proc Natl Acad Sci USA. 2000; 97:2962–2964. [PubMed: 10737776]

Johnson E, Palmer AG, Rance M. Temperature dependence of the NMR generalized order parameter. Proteins Struct Funct Bioinform. 2007; 66:796–803.

Kay LE, Ikura M, Tschudin R, Bax A. 3-Dimensional triple-resonance NMR-spectroscopy of isotopically enriched proteins. J Magn Reson. 1990; 89:496–514.

Krizova H, Zidek L, Stone MJ, Novotny MV, Sklenar V. Temperature-dependent spectral density analysis applied to monitoring backbone dynamics of major urinary protein-I complexed with the pheromone 2-sec-butyl-4, 5-dihydrothiazole. J Biom NMR. 2004; 28:369–384.

Kubelka J, Chiu TK, Davies DR, Eaton WA, Hofrichter J. Sub-microsecond protein folding. J Mol Biol. 2006; 359:546–553. [PubMed: 16643946]

Lipari G, Szabo A. Model-free approach to the interpretation of nuclear magnetic-resonance relaxation in macromolecules. 1. Theory and range of validity. J Am Chem Soc. 1982; 104:4546–4559.

Loth K, Pelupessy P, Bodenhausen G. Chemical shift anisotropy tensors of carbonyl, nitrogen, and amide proton nuclei in proteins through cross-correlated relaxation in NMR spectroscopy. J Am Chem Soc. 2005; 127:6062–6068. [PubMed: 15839707]

Mandel AM, Akke M, Palmer AG. Backbone dynamics of *Escherichia-coli* ribonuclease Hi—correlations with structure and function in an active enzyme. J Mol Biol. 1995; 246:144–163. [PubMed: 7531772]

Mandel AM, Akke M, Palmer AG. Dynamics of ribonuclease H: temperature dependence of motions on multiple time scales. Biochemistry. 1996; 35:16009–16023. [PubMed: 8973171]

Massi F, Palmer AG. Temperature dependence of NMR order parameters and protein dynamics. J Am Chem Soc. 2003; 125:11158–11159. [PubMed: 16220912]

McKnight CJ, Doering DS, Matsudaira PT, Kim PS. A thermostable 35-residue subdomain within villin headpiece. J Mol Biol. 1996; 260:126–134. [PubMed: 8764395]

Meirovitch E, Polimeno A, Freed JH. Comment on "The physical basis of model-free analysis of NMR relaxation data from proteins and complex fluids". J Chem Phys. 2009; 132:207101–207102. [PubMed: 20515116]

Meirovitch E, Shapiro YE, Pohmeno A, Freed JH. Structural dynamics of bio-macromolecules by NMR: the slowly relaxing local structure approach. Prog Nucl Magn Reson Spec. 2010; 56:360–405.

Mosteller, F.; Tukey, JW. Data analysis and regression: a second course in statistics. Addison-Wesley; Reading: 1977.

Orekhov VY, Pervushin KV, Arseniev AS. Backbone dynamics of (1–71)bacterioopsin studied by 2-dimensional H-1-N-15 NMR-spectroscopy. Eur J Biochem. 1994; 219:887–896. [PubMed: 8112340]

Pang Y, Buck M, Zuiderweg ERP. Backbone dynamics of the ribonuclease binase active site area using multinuclear (N-15 and (CO)-C-13) NMR relaxation and computational molecular dynamics. Biochemistry. 2002; 41:2655–2666. [PubMed: 11851412]

Pelupessy P, Minguez Espallargas G, Bodenhausen G. Symmetrical reconversion: measuring cross-correlation rates with enhanced accuracy. J Magn Reson. 2003; 161:258–264. [PubMed: 12713978]

Pelupessy P, Ferrage F, Bodenhausen G. Accurate measurement of longitudinal cross-relaxation rates in nuclear magnetic resonance. J Chem Phys. 2007; 126:134508. [PubMed: 17430048]

Schuler B, Kremer W, Kalbitzer HR, Jaenicke R. Role of entropy in protein thermostability: folding kinetics of a hyper-thermophilic cold shock protein at high temperatures using F-19 NMR. Biochemistry. 2002; 41:11670–11680. [PubMed: 12269809]

Seewald MJ, Pichumani K, Stowell C, Tibbals BV, Regan L, Stone MJ. The role of backbone conformational heat capacity in protein stability: temperature dependent dynamics of the B1 domain of Streptococcal protein G. Protein Sci. 2000; 9:1177–1193. [PubMed: 10892810]

Spyracopoulos L, Lavigne P, Crump MP, Gagne SM, Kay CM, Sykes BD. Temperature dependence of dynamics and thermodynamics of the regulatory domain of human cardiac troponin C. Biochemistry. 2001; 40:12541–12551. [PubMed: 11601978]

Tang Y, Grey MJ, McKnight J, Palmer AG, Raleigh DP. Multistate folding of the villin headpiece domain. J Mol Biol. 2006; 355:1066–1077. [PubMed: 16337228]

Thurber KR, Tycko R. Biomolecular solid state NMR with magic-angle spinning at 25K. J Magn Reson. 2008; 195:179–186. [PubMed: 18922715]

Tugarinov V, Liang ZC, Shapiro YE, Freed JH, Meirovitch E. A structural mode-coupling approach to N-15 NMR relaxation in proteins. J Am Chem Soc. 2001; 123:3055–3063. [PubMed: 11457016]

Vugmeyster L, McKnight CJ. Slow motions in chicken Villin Headpiece subdomain probed by cross-correlated NMR relaxation of amide NH bonds in successive residues. Biophys J. 2008; 95:5941–5950. [PubMed: 18820237]

Vugmeyster L, Trott O, McKnight CJ, Raleigh DP, Palmer AG. Temperature-dependent dynamics of the villin headpiece helical subdomain, an unusually small thermostable protein. J Mol Biol. 2002; 320:841–854. [PubMed: 12095260]

Vugmeyster L, Raleigh DP, Palmer AG, Vugmeister BE. Beyond the decoupling approximation in the model free approach for the interpretation of NMR relaxation of macromolecules in solution. J Am Chem Soc. 2003; 125:8400–8404. [PubMed: 12837113]

Vugmeyster L, Ostrovsky D, Ford JJ, Burton SD, Lipton AS, Hoatson GL, Vold RL. Probing the dynamics of a protein hydrophobic core by deuteron solid-state nuclear magnetic resonance spectroscopy. J Am Chem Soc. 2009; 131:13651–13658. [PubMed: 19772361]

Vugmeyster L, Ostrovsky D, Li Y. Comparison of fast backbone dynamics at amide nitrogen and carbonyl sites in dematin headpiece C-terminal domain and its S74E mutant. J Biom NMR. 2010; 47:155–162.

Wand AJ. Dynamic activation of protein function: a view emerging from NMR spectroscopy. Nat Struct Biol. 2001; 8:926–931. [PubMed: 11685236]

Wang MH, Tang YF, Sato SS, Vugmeyster L, McKnight CJ, Raleigh DP. Dynamic NMR line-shape analysis demonstrates that the villin headpiece subdomain folds on the microsecond time scale. J Am Chem Soc. 2003a; 125:6032–6033. [PubMed: 12785814]

Wang TZ, Cai S, Zuiderweg ERP. Temperature dependence of anisotropic protein backbone dynamics. J Am Chem Soc. 2003b; 125:8639–8643. [PubMed: 12848571]

Wang TZ, Frederick KK, Igumenova TI, Wand AJ, Zuiderweg ERP. Changes in calmodulin main-chain dynamics upon ligand binding revealed by cross-correlated NMR relaxation measurements. J Am Chem Soc. 2005; 127:828–829. [PubMed: 15656608]

Wang T, Weaver DS, Cai S, Zuiderweg ERP. Quantifying Lipari–Szabo modelfree parameters from 13CO NMR relaxation experiments. J Biom NMR. 2006; 36:79–102.

Wickstrom L, Okur A, Song K, Hornak V, Raleigh DP, Simmerling CL. The unfolded state of the villin headpiece helical subdomain: computational studies of the role of locally stabilized structure. J Mol Biol. 2006; 360:1094–1107. [PubMed: 16797585]

Wickstrom L, Bi Y, Hornak V, Raleigh DP, Simmerling C. Reconciling the solution and X-ray structures of the villin headpiece helical subdomain: molecular dynamics simulations and double mutant cycles reveal a stabilizing cation-pi interaction. Biochemistry. 2007; 46:3624–3634. [PubMed: 17338549]

Xiao SF, Bi Y, Shan B, Raleigh DP. Analysis of core packing in a cooperatively folded miniature protein: the ultrafast folding Villin Headpiece helical subdomain. Biochemistry. 2009; 48:4607–4616. [PubMed: 19354264]

Yang DW, Mok YK, FormanKay JD, Farrow NA, Kay LE. Contributions to protein entropy and heat capacity from bond vector motions measured by NMR spin relaxation. J Mol Biol. 1997; 272:790–804. [PubMed: 9368658]
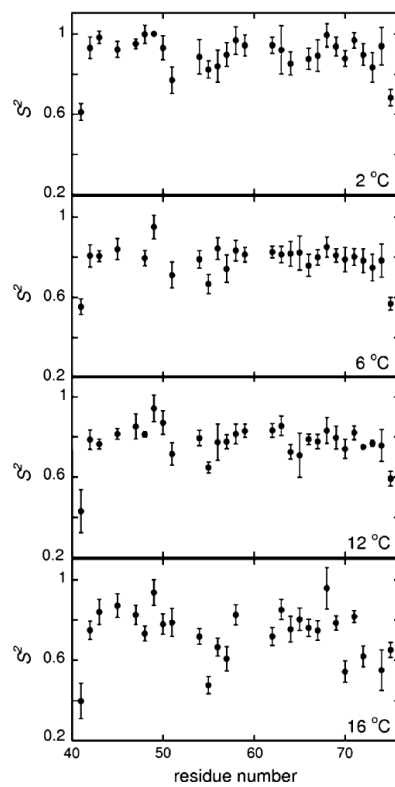
Fig. 1.
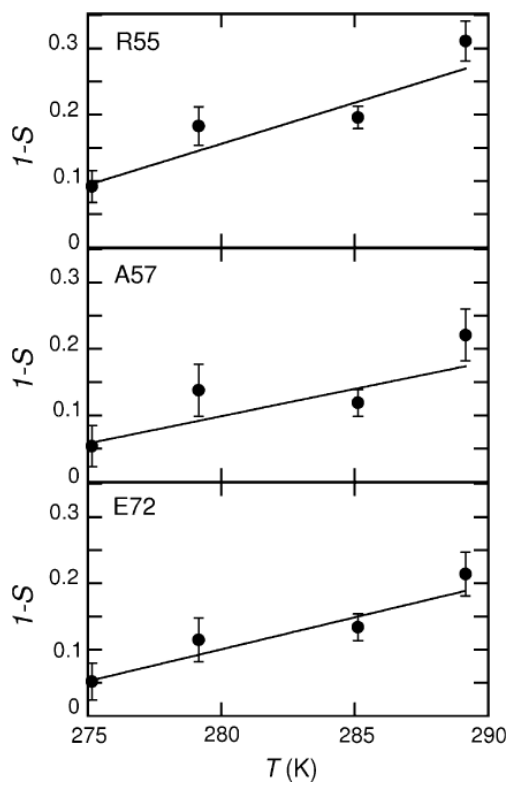Plots of order parameters versus residue number. The numbering of residues in HP36 starts with #41

Fig. 2.
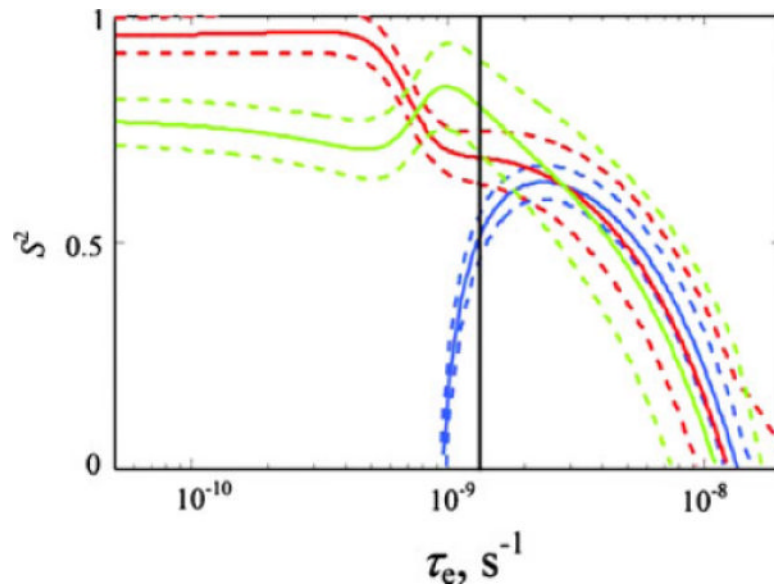Sample plots of $1 - S$ versus T

Fig. 3.
A representative plot showing the range of S^2 and τ_e values consistent with the experimental rates. The data are shown for T54 at 22°C. *Solid lines* represent S^2 and τ_e values that fit R_1 (*blue*), $R_{C'/C'-C\alpha}$ (*green*) and $R_{C'/C'-N}$ (*red*) relaxation rates. *Dotted lines* mark the area of the parameters that fit the rates within the limits of the experimental errors. The *black vertical line* represents the boundary $\tau_e = \tau_c 2$: The angle θ was fixed by the following procedure: for each value of τ_e, the χ^2 function was minimized with the respect to S^2 and θ. The resulting value of θ was then used to calculate S^2 which reproduces the experimental values of $R_{C'/C'-C\alpha}$ and $R_{C'/C'-N}$ rates for a given τ_e

Table 1

The values of slopes of 1-S versus T plots

Residue	Slope (1/K) × 10^3	Residue	Slope (1/K) × 10^3
41	11.1 ± 1.0	62	6.6 ± 3.0
42	6.4 ± 1.9	63	−1.6 ± 1.8
43	8.3 ± 4.7	64	6.1 ± 1.9
45	3.7 ± 2.4	65	0.7 ± 5.1
47	4.8 ± 0.2	66	3.4 ± 2.2
48	7.2 ± 3.7	67	4.1 ± 1.5
49	2.7 ± 0.7	68	3.8 ± 5.0
50	5.5 ± 2.0	69	4.5 ± 2.6
51	−0.3 ± 2.6	70	11.7 ± 3.1
54	4.7 ± 2.2	71	4.8 ± 3.0
55	12.3 ± 3.9	72	8.3 ± 2.8
56	8.4 ± 1.9	73	2.9 ± 2.2
57	8.3 ± 4.4	74	12.8 ± 4.1
58	4.2 ± 2.7	75	0.5 ± 3.9
59	4.2 ± 5.3		

Table 2

Analysis of the sensitivity of the fits to τ_e boundary

	2°C	6°C	12°C	16°C	22°C
Average ($|S^2 (\tau_c/2) - S^2 (\tau_c/3)|$)	0.0038	0.0036	0.011	0.022	0.060
Median $\chi^2 (\tau_c/2)$	0.98	0.058	0.54	1.1	1.8
Median ($\chi^2 (\tau_c/3) - \chi^2 (\tau_c/2)$)	0.020	0.15	1.2	3.8	10

The values in brackets represent the upper limit of constraints imposed on the values of τ_e in the fitting procedure